

# Synthesis, crystal structures and properties of six cubane-like transition metal complexes of di-2-pyridyl ketone in *gem*-diol form

Ming-Liang Tong,<sup>\*a,b</sup> Shao-Liang Zheng,<sup>a</sup> Jian-Xin Shi,<sup>a</sup> Ye-Xiang Tong,<sup>a</sup> Hung Kay Lee<sup>c</sup> and Xiao-Ming Chen<sup>\*a</sup>

<sup>a</sup> State Key Laboratory of Optoelectronic Materials & Technologies and School of Chemistry & Chemical Engineering, Zhongshan University, Guangzhou 510275, P. R. China.  
E-mail: cestml@zsu.edu.cn (M.-L. Tong) & cescxm@zsu.edu.cn (X.-M. Chen)

<sup>b</sup> State Key Laboratory of Structural Chemistry, Fujian Institute of Research on the Structure of Matter, Chinese Academy of Sciences, Fuzhou 350002, P. R. China

<sup>c</sup> Department of Chemistry, The Chinese University of Hong Kong, Shatin, New Territories, Hong Kong, P. R. China

Received 17th December 2001, Accepted 4th February 2002

First published as an Advance Article on the web 20th March 2002

Six cubane-type complexes comprising similar  $[M_4O_4]^{n+}$  cores [ $M = Mn(\text{II}), Co(\text{II}), Ni(\text{II}), Zn(\text{II})$  or  $Cd(\text{II})$ ] synthesised in a facile route utilizing the *gem*-diol form of di-2-pyridyl ketone as a ligand have been characterised by X-ray structural analysis. Complex **1** crystallizes in the cubic space group  $I\bar{4}3d$ , which is the highest symmetry documented in the cubane-like manganese compounds to date, while the other complexes crystallize in much lower crystallographic symmetries. The four metal ions and bridging alkoxo oxygen atoms are located at alternating vertices of a cube, with either pyridyl, acetate or aqua groups on the exterior of the core. Variable temperature magnetic susceptibility measurements indicate the presence of an antiferromagnetic behavior in **2** and ferromagnetic behaviors in **3** and **6**. The temperature dependence of the magnetic susceptibility for **6** was fitted with  $J_1 = 6.04 \text{ cm}^{-1}$ ,  $J_2 = -1.47 \text{ cm}^{-1}$ , and  $g = 2.12$ . The difference in sign between the  $J_1$  and  $J_2$  superexchange interactions is in good agreement with the different types of faces present in this  $Ni_4O_4$  cubane core. Both **4** and **5** show similar ambient and cryogenic temperature emissions in solid state.

## Introduction

Recently, considerable research effort has been focused on studies of cubane-type polynuclear complexes due to their relevance to multi-electron transfer centres in biological systems,<sup>1</sup> and to their interesting magnetic and optical properties,<sup>2,3</sup> as well as to their potential relevance to inorganic solids.<sup>4</sup> Although cubane-type complexes of the type  $Fe_4S_4$  or  $Mn_4O_4$  and their derivatives have been extensively investigated,<sup>1,5</sup> reports on complexes containing  $Zn_4$  and  $Cd_4$  cubane cores are rare. We reported the first cubane-like zinc(II) and cadmium(II) complexes in a previous communication,<sup>6</sup> thereafter, another two cubane-like zinc(II) complexes have been documented.<sup>7</sup>

On the other hand, di-2-pyridyl ketone  $[(C_5H_4N)_2CO, dpk]$  and its hydrolyzed derivative  $[(C_5H_4N)_2C(OH)_2, dpd]$  are good chelating ligands, and a few polynuclear complexes of the monoanion or dianion of the *gem*-diol form of di-2-pyridyl ketone ( $dpg - H$  and  $dpg - 2H$ ) obtained from metal carboxylates and dpk have been isolated and structurally characterized.<sup>8-10</sup> We report here a systematic preparation, structures and physical properties of six discrete cubane-type  $Mn(\text{II})$ ,  $Co(\text{II})$ ,  $Ni(\text{II})$ ,  $Zn(\text{II})$  and  $Cd(\text{II})$  complexes using the mono-anionic  $dpg - H$  as a ligand, namely,  $[Mn_4(dpg - H)_4Cl_4] \cdot H_2O$  (**1**),  $[M_4(dpg - H)_4(O_2CMe)_m(H_2O)_n](ClO_4)_{4-m} \cdot xH_2O$  (**2**:  $M = Mn^{2+}$ ,  $m = 3$ ,  $n = 1$ ; **3**:  $M = Co^{2+}$ ,  $m = 3$ ,  $n = 1$ ; **4**:  $M = Zn^{2+}$ ,  $m = n = 2$ ; **5**:  $M = Cd^{2+}$ ,  $m = 3$ ,  $n = 1$ ; and **6**:  $M = Ni^{2+}$ ,  $m = 3$ ,  $n = 0$ ).

## Experimental

All reagents were used as received from commercial sources. The C, H, N microanalyses were carried out with a Perkin-

Elmer 240 elemental analyzer. EPR spectra were recorded on a Bruker EMX spectrometer operating at X-band and equipped with a variable temperature helium flow cryostat system (Oxford Instruments). For low-temperature photoluminescence measurement, samples were mounted in a closed-cycle cryostat in which temperature can be adjusted from 10 to 300 K. The 325 nm line of a He-Cd laser was used as an excitation source. The emission light was collected and dispersed by a 0.25 m double-monochromator with a water-cooled photomultiplier tube and processed with a lock-in amplifier. The room-temperature emission and excitation spectra were carried out using a Hitachi F-4500 spectrofluorometer. Variable-temperature magnetic susceptibility data were obtained from a Quantum Design SQUID magnetometer. Experimental magnetic susceptibility data were corrected from diamagnetism of the constituent atoms.<sup>11</sup> The effective molar magnetic moments were calculated with the equation  $\mu_{eff} = 2.828(\chi_M T)^{1/2}$ .

**Caution:** Perchlorate salts of metal complexes with organic ligands are potentially explosive. Only small amounts of material should be prepared and these should be handled with great caution.

## Syntheses

**Synthesis of  $[Mn_4(dpg - H)_4Cl_4] \cdot H_2O$  (1).** An acetonitrile solution (10 cm<sup>3</sup>) of dpk (0.092 g, 0.5 mmol) was added dropwise to a stirring aqueous solution (5 cm<sup>3</sup>) of  $MnCl_2 \cdot 4H_2O$  (0.144 g, 1.0 mmol) at room temperature for 15 min. A solution (5 cm<sup>3</sup>) of NaOH (0.04 g, 1.0 mmol) was then added dropwise. The resulting solution was allowed to stand in air at room temperature for two weeks, yielding polyhedral colorless crystals (ca. 85% yield based on dpk). IR (KBr, cm<sup>-1</sup>): 3535m,

3367s, 3071m, 2804w, 1602vs, 1567m, 1475m, 1440m, 1377m, 1321w, 1300m, 1257w, 1222m, 1159w, 1110m, 1082vs, 1046vs, 1018s, 948m, 899m, 800m, 779m, 758m, 681m, 639m, 589m, 526w, 456m. Calc. for  $C_{44}H_{38}N_8O_9Cl_4Mn_4$ : C, 44.62; H, 3.23; N, 9.46%. Found: C, 44.54; H, 3.16; N, 9.34%.

**Synthesis of  $[Mn_4(dp\text{-H})_4(O_2CMe)_3(H_2O)](ClO_4)\cdot H_2O$  (2).** An acetonitrile solution ( $10\text{ cm}^3$ ) of dpk (0.092 g, 0.5 mmol) was added dropwise to a stirring aqueous solution ( $5\text{ cm}^3$ ) of  $Mn(O_2CMe)_2\cdot 4H_2O$  (0.245 g, 1.0 mmol) at  $50^\circ\text{C}$  for 15 min. A solution ( $10\text{ cm}^3$ ) of  $NaClO_4$  (0.142 g, 1.0 mmol) was then added. The resulting solution was allowed to stand in air at room temperature for two weeks, yielding pale yellow polyhedral crystals (*ca.* 75% yield based on dpk). IR (KBr,  $\text{cm}^{-1}$ ): 3353m, 3085m, 2818w, 1595vs, 1475m, 1433s, 1335m, 1300m, 1257w, 1222m, 1152w, 1117s, 1082vs, 1053vs, 1018m, 948m, 807m, 779m, 758m, 681m, 653m, 589m, 526w, 456m, 407w. Calc. for  $C_{50}H_{49}N_8O_{20}ClMn_4$ : C, 44.9; H, 3.7; N, 8.4%. Found: C, 44.9; H, 3.6; N, 8.3%.

**Synthesis of  $[Co_4(dp\text{-H})_4(O_2CMe)_3(H_2O)](ClO_4)\cdot 1.8H_2O$  (3).** This was prepared as for 2. (*ca.* 75% yield based on dpk). IR (KBr,  $\text{cm}^{-1}$ ): 3353m, 3085m, 2825w, 2678w, 1602vs, 1574s, 1468m, 1419vs, 1335m, 1293w, 1222m, 1110s, 1082vs, 1018m, 955w, 899w, 807m, 772m, 681m, 653m, 625m, 596w, 505w, 477m. Calc. for  $C_{50}H_{50.6}N_8O_{20.8}ClCo_4$ : C, 43.9; H, 3.7; N, 8.2%. Found: C, 43.8; H, 3.6; N, 8.1%.

**Synthesis of  $[Zn_4(dp\text{-H})_4(O_2CMe)_2(H_2O)](ClO_4)\cdot 6.5H_2O$  (4).** This was prepared as for 2. (*ca.* 72% yield based on dpk). IR (KBr,  $\text{cm}^{-1}$ ): 3360m, 2818w, 1602vs, 1475m, 1440s, 1384m, 1328m, 1300w, 1264w, 1222m, 1117vs, 1089vs, 1053s, 1025s, 955m, 906w, 800m, 772m, 758m, 681m, 660w, 632w, 596w, 491w, 463w, 407w. Calc. for  $C_{48}H_{57}N_8O_{27.5}Cl_2Zn_4$ : C, 38.0; H, 3.8; N, 7.4%. Found: C, 37.6; H, 3.5; N, 7.1%.

**Synthesis of  $[Cd_4(dp\text{-H})_4(O_2CMe)_3](ClO_4)\cdot 2H_2O$  (5).** This was prepared as for 2. (*ca.* 90% yield based on dpk). IR (KBr,  $\text{cm}^{-1}$ ): 3550w, 3332m, 3107m, 1595vs, 1574vs, 1475m, 1433s, 1412s, 1335w, 1300w, 1257w, 1222m, 1152w, 1089vs, 1053s, 1018s, 948m, 800m, 779m, 758m, 674m, 639m, 589w, 449w. Calc. for  $C_{50}H_{49}N_8O_{20}ClCd_4$ : C, 38.3; H, 3.2; N, 7.2%. Found: C, 38.1; H, 3.0; N, 7.0%.

**Synthesis of  $[Ni_4(dp\text{-H})_4(O_2CMe)_3(H_2O)](ClO_4)\cdot 8.25H_2O$  (6).** This was prepared as for 2. (*ca.* 80% yield based on dpk). IR (KBr,  $\text{cm}^{-1}$ ): 3423s, br, 3081m, 2832w, 1602vs, 1581vs, 1433vs, 1398s, 1335m, 1293w, 1257w, 1215m, 1159w, 1117s, 1089vs, 1053s, 1025m, 955m, 906w, 807m, 765m, 681m, 617m, 647w, 512w, 470w, 421w. Calc. for  $C_{50}H_{63.5}N_8O_{27.25}ClNi_4$ : C, 40.5; H, 4.3; N, 7.6%. Found: C, 40.5; H, 4.2; N, 7.5%.

## X-Ray crystallography

Diffraction intensities for the six complexes were collected at  $21^\circ\text{C}$  on a Siemens R3m diffractometer using the  $\omega$ -scan technique. Lorentz-polarization and absorption corrections were applied.<sup>12</sup> The structures were solved with direct methods and refined with full-matrix least-squares technique using the SHELXS-97 and SHELXL-97 programs, respectively.<sup>13,14</sup> Non-hydrogen atoms were refined anisotropically. The organic hydrogen atoms were generated geometrically (C–H = 0.96 Å); the aqua hydrogen atoms were located from difference maps and refined with isotropic temperature factors. Analytical expressions of neutral-atom scattering factors were employed, and anomalous dispersion corrections were incorporated.<sup>15</sup> The absolute structure for 1 has been determined with a Flack parameter of  $-0.05(7)$ .<sup>16</sup> The crystallographic data for 1–6 are listed in Table 1. Selected interatomic contacts (Å) and bond angles (°) for 1–6 are given in Tables 2–7, respectively. Drawings were produced with SHELXTL.<sup>17</sup>

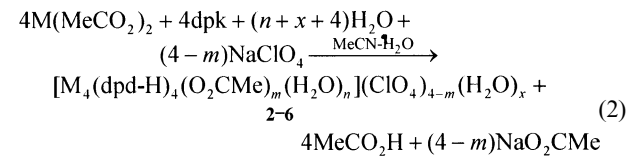
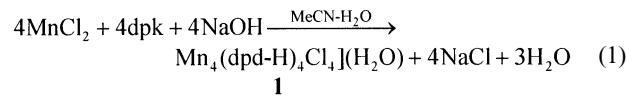
CCDC reference numbers 144515–144519 and 170212.

See <http://www.rsc.org/suppdata/dt/b1/b111475c/> for crystallographic data in CIF or other electronic format.

## Results and discussion

### Synthesis

The preparation of compounds 1–6 can be achieved *via* the 1 : 0.5 reaction of  $MnCl_2$  or  $M(O_2CMe)_2$  with dpk in MeCN– $H_2O$ . This preparation can be summarized by eqns. (1) and (2).



For 2: M =  $Mn^{2+}$ , m = 3, n = 1; 3 : M =  $Co^{2+}$ , m = 3, n = 1; 4 : M =  $Mn^{2+}$ , m = n = 2; 5 : M =  $Cd^{2+}$ , m = 3, n = 1; and 6 : M =  $Ni^{2+}$ , m = 3, n = 0

### Crystal structures

1 is made up of neutral cubane-type  $[Mn_4(dp\text{-H})_4Cl_4]$  species and lattice water molecules. Within each  $[Mn_4(dp\text{-H})_4Cl_4]$ , the four Mn(II) atoms are crystallographically equivalent, and each is coordinated to three oxygen atoms and two nitrogen atoms from different dpd – H ligands, and further ligated by a chloride ion, completing a distorted octahedral geometry at Mn(II) (Fig. 1, Table 2). Each cubane core is constructed by four Mn(II) atoms and four oxygen atoms from the four dpd – H ligands each at alternating corners, where the four Mn(II) atoms are crystallographically equivalent and each is coordinated to three  $\mu_3$ -alkxo oxygen atoms and two nitrogen atoms from three dpd – H ligands, and is further ligated by a chloride ion, completing an octahedral coordination at Mn(II). Another oxygen atom of each dpd – H ligand remains protonated and unbound to metal ions. Hence the resulting mono-anion acts as a  $\eta^1\cdot\eta^3\cdot\eta^1\cdot\mu_3$  ligation mode, which has recently been reported in a double cubane complex,<sup>7a</sup> but different from those found in most metal complexes of dpd – H.<sup>7</sup> The Mn–O, Mn–N, and Mn ··· Mn distances are 2.159(4)–2.292(4), 2.228(5) and 3.350(4)–3.412(4) Å, respectively, which are consistent with those reported for related complexes.<sup>5b,18</sup>

It is interesting to note that each chloride ion in  $Mn_4(dp\text{-H})_4Cl_4$  species forms an acceptor hydrogen bond with the adjacent water molecule [O ··· Cl 3.042(5) Å], and each lattice water molecule forms two donor hydrogen bonds with two adjacent chloride ions from two different  $[Mn_4(dp\text{-H})_4Cl_4]$  species. Therefore, each  $[Mn_4(dp\text{-H})_4Cl_4]$  species contacts with four  $[Mn_4(dp\text{-H})_4Cl_4]$  ones through Cl ··· O(w) ··· Cl hydrogen bonding interaction (Fig. 2(a)), resulting in an interesting three-dimensional hydrogen-bonded diamond network (Fig. 2(b)).

A few Mn(I,II) cubane structures with formulae  $[Mn_4(CO)_{12}(F\text{ or }OH)_4]^{19a,b}$ ,  $[Mn_4(CO)_{12}(OR)_4]^{19c}$  and those containing  $[Mn_4(alkoxy)_4]$  cores<sup>5b,19d,e</sup> have been reported previously. To our knowledge, however, 1 present here is the first example with high symmetry to date.

The structures of 2 and 3 are almost isostructural (Fig. 3(a) and (b), Tables 3 and 4) the only minor difference being the contents of lattice water molecules. Each cubane core in 2 or 3 is constructed by four metal(II) atoms and four oxygen atoms

**Table 1** Crystal data and structure refinement for **1–6**

	<b>1</b>	<b>2</b>	<b>3</b>	<b>4</b>	<b>5</b>	<b>6</b>
Formula	$C_{44}H_{38}Cl_4Mn_4\cdot$ $N_8O_9$	$C_{50}H_{49}ClMn_4\cdot$ $N_8O_{20}$	$C_{50}H_{50.5}ClCo_4\cdot$ $N_8O_{20.8}$	$C_{48}H_{57}Cl_2N_8\cdot$ $O_{27.5}Zn_4$	$C_{50}H_{49}Cd_4Cl\cdot$ $N_8O_{20}$	$C_{50}H_{63.5}ClN_8\cdot$ $Ni_4O_{27.25}$
$M_w$	1184.38	1337.18	1367.45	1518.40	1567.02	1482.87
Crystal system	Cubic	Triclinic	Triclinic	Monoclinic	Triclinic	Monoclinic
Space group	$I\bar{4}3d$	$P\bar{1}$	$P\bar{1}$	$P2_1/n$	$P\bar{1}$	$P2_1/c$
$a/\text{\AA}$	24.287(6)	12.927(8)	12.893(11)	15.328(6)	13.065(4)	11.943(3)
$b/\text{\AA}$	24.287(6)	14.245(10)	14.228(11)	24.181(12)	14.315(8)	24.582(8)
$c/\text{\AA}$	24.287(6)	15.943(7)	16.048(8)	16.060(8)	16.082(8)	21.892(9)
$\alpha^\circ$		89.84(1)	89.43(1)		90.53(1)	
$\beta^\circ$		72.58(1)	72.39(1)	97.25(1)	108.10(1)	100.60(1)
$\gamma^\circ$		86.02(1)	86.61(1)		93.94(1)	
$V/\text{\AA}^3$	14326(6)	2794(3)	2801(3)	5905(5)	2851(2)	6317(4)
$Z$	12	2	2	4	2	4
$D_\rho/\text{g cm}^{-3}$	1.647	1.589	1.621	1.708	1.826	1.558
$T/\text{^\circ C}$	20(2)	20(2)	20(2)	20(2)	20(2)	20(2)
$\mu(\text{Mo-K}\alpha)/\text{mm}^{-1}$	1.321	1.014	1.297	1.791	1.600	1.305
No. unique data	1139	9827	11000	10386	11210	11116
No. data with $I > 2\sigma(I)$	886	7311	8313	5626	7500	6402
$R_1, wR_2^a$	0.0468, 0.1280	0.0464, 0.1255	0.0431, 0.1070	0.0637, 0.1533	0.0896, 0.2674	0.0738, 0.2259

<sup>a</sup>  $R_1 = \sum \|F_o\| - |F_c| \|/ \sum |F_o\|$ ,  $wR_2 = [\sum w(F_o^2 - F_c^2)^2 / \sum w(F_o^2)^2]^{1/2}$ ,  $w = [\sigma^2(F_o)^2 + (0.1(\max(0, F_o^2) + 2F_c^2)/3)^2]^{-1}$ .

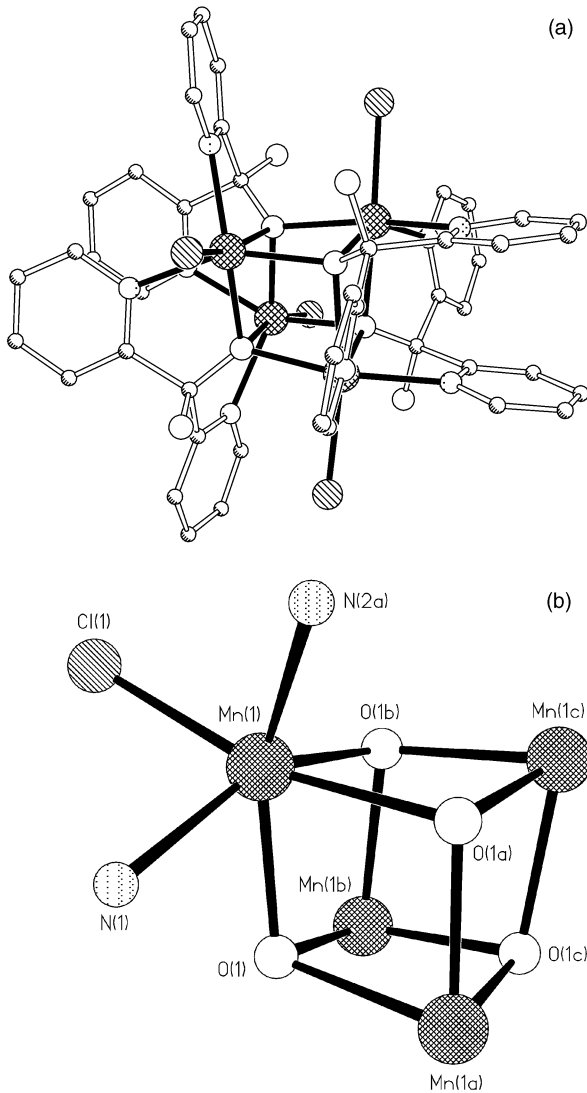


**Fig. 1** Perspective view of the cubane core (a) and bridging skeleton of the four Mn(II) atoms in the cubane core (b) in **1**.

each from a dpd – H ligand and each at alternating corners. Each Mn(II) atom is coordinated in a distorted octahedral geometry by three  $\mu_3$ -alkoxo oxygen atoms and two nitrogen atoms from three dpd – H ligands. Besides the three oxygen

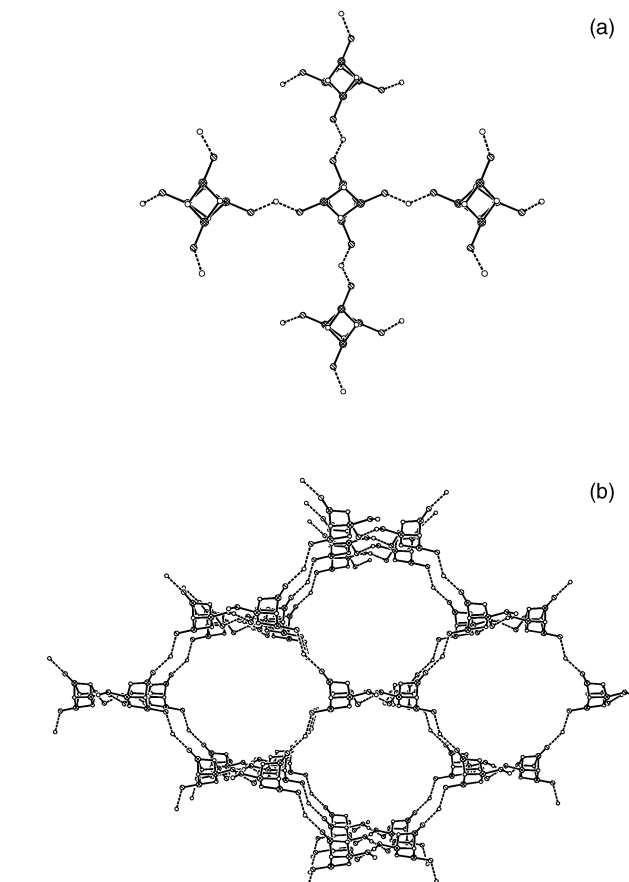


**Fig. 2** Perspective view of the hydrogen bonding between the cubane cores (a) and the hydrogen-bonded supramolecular network (b) in **1**.

atoms each from a dpd – H ligand, the fourth oxygen atom is from a monodentate acetate group for the three metal atoms, and is from an aqua ligand for the remaining metal atom. The M–O(alkoxo) distances are in the range 2.156(3)–2.312(3) and 1.998(3)–2.062(3) Å for **2** and **3**, respectively, which are in accord with the sequence of the radii of their metal ions. The M · · · M separations in **2** and **3** are 3.317–3.413 and 3.208–3.279 Å, comparable to those found in related complexes.<sup>5b,9</sup>

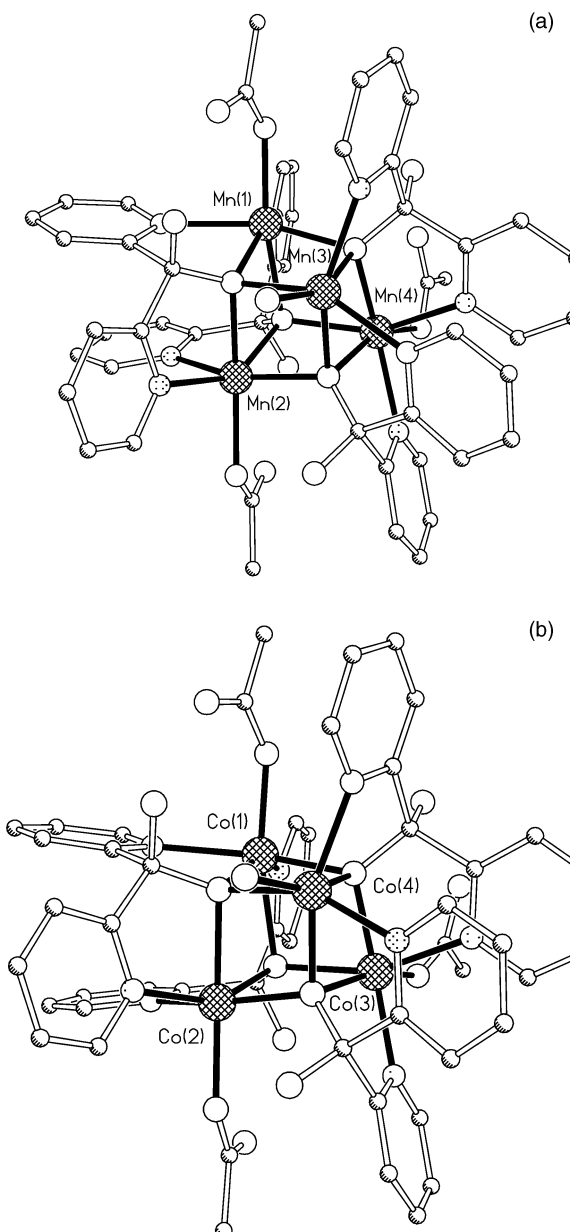
The structures of **4** and **5** are very similar (Fig. 4, Tables 5 and 6). Each cubane core in **4** is constructed by four Zn(II) atoms

**Table 2** Selected interatomic contacts ( $\text{\AA}$ ) and bond angles ( $^\circ$ ) for **1**

Mn(1)–O(1)	2.159(4)	Mn(1)–O(1b)	2.292(4)
Mn(1)–O(1a)	2.182(3)	Mn(1)–Cl(1)	2.445(2)
Mn(1)–N(2b)	2.228(5)	Cl(1) ··· O(1w)	3.042(5)
O(1)–Mn(1)–O(1a)	81.6(1)	N(2b)–Mn(1)–O(1b)	71.3(2)
O(1)–Mn(1)–N(2b)	146.7(2)	N(1)–Mn(1)–O(1b)	99.6(1)
O(1a)–Mn(1)–N(2b)	107.0(2)	O(1)–Mn(1)–Cl(1)	113.1(1)
O(1)–Mn(1)–N(1)	72.3(1)	O(1a)–Mn(1)–Cl(1)	95.8(1)
O(1a)–Mn(1)–N(1)	153.6(2)	N(2b)–Mn(1)–Cl(1)	98.3(2)
N(2b)–Mn(1)–N(1)	97.1(2)	N(1)–Mn(1)–Cl(1)	91.3(1)
O(1)–Mn(1)–O(1b)	79.3(1)	O(1b)–Mn(1)–Cl(1)	165.7(1)
O(1a)–Mn(1)–O(1b)	78.6(1)		

Symmetry codes: *a*)  $y + 1/4, -x + 7/4, -z + 5/4$ ; *b*)  $-x + 2, -y + 3/2, z$ .**Table 3** Selected interatomic contacts ( $\text{\AA}$ ) and bond angles ( $^\circ$ ) for **2**

Mn(1)–O(9)	2.082(3)	Mn(3)–O(1)	2.165(3)
Mn(1)–O(3)	2.162(3)	Mn(3)–O(3)	2.207(3)
Mn(1)–O(1)	2.186(3)	Mn(3)–O(7)	2.169(3)
Mn(1)–N(5)	2.215(3)	Mn(3)–O(1w)	2.174(3)
Mn(1)–N(1)	2.279(3)	Mn(3)–N(3)	2.250(3)
Mn(1)–O(5)	2.306(3)	Mn(3)–N(7)	2.202(3)
Mn(2)–O(11)	2.119(3)	Mn(4)–O(3)	2.206(3)
Mn(2)–O(5)	2.156(3)	Mn(4)–O(5)	2.163(3)
Mn(2)–O(7)	2.157(3)	Mn(4)–O(7)	2.312(3)
Mn(2)–N(2)	2.227(3)	Mn(4)–O(13)	2.114(5)
Mn(2)–N(6)	2.232(3)	Mn(4)–N(4)	2.257(4)
Mn(2)–O(1)	2.286(3)	Mn(4)–N(8)	2.240(4)
O(9)–Mn(1)–O(3)	101.1(1)	O(1)–Mn(3)–O(7)	80.9(1)
O(9)–Mn(1)–O(1)	116.0(1)	O(1)–Mn(3)–O(1w)	89.9(1)
O(3)–Mn(1)–O(1)	80.0(1)	O(7)–Mn(3)–O(1w)	117.6(1)
O(9)–Mn(1)–N(5)	94.8(1)	O(1)–Mn(3)–N(7)	151.8(1)
O(3)–Mn(1)–N(5)	110.6(1)	O(7)–Mn(3)–N(7)	73.4(1)
O(1)–Mn(1)–N(5)	145.4(1)	O(1w)–Mn(3)–N(7)	91.7(1)
O(9)–Mn(1)–N(1)	89.6(1)	O(1)–Mn(3)–O(3)	79.5(1)
O(3)–Mn(1)–N(1)	151.7(1)	O(7)–Mn(3)–O(3)	80.3(1)
O(1)–Mn(1)–N(1)	71.7(1)	O(1w)–Mn(3)–O(3)	157.7(1)
N(5)–Mn(1)–N(1)	94.4(1)	N(7)–Mn(3)–O(3)	107.0(1)
O(9)–Mn(1)–O(5)	164.5(1)	O(1)–Mn(3)–N(3)	107.9(1)
O(3)–Mn(1)–O(5)	77.2(1)	O(7)–Mn(3)–N(3)	149.7(1)
O(1)–Mn(1)–O(5)	79.1(1)	O(1w)–Mn(3)–N(3)	91.9(1)
N(5)–Mn(1)–O(5)	71.9(1)	N(7)–Mn(3)–N(3)	100.2(1)
N(1)–Mn(1)–O(5)	99.0(1)	O(3)–Mn(3)–N(3)	73.2(1)
O(11)–Mn(2)–O(5)	122.0(1)	O(13)–Mn(4)–O(5)	105.6(1)
O(11)–Mn(2)–O(7)	92.2(1)	O(13)–Mn(4)–O(3)	124.4(1)
O(5)–Mn(2)–O(7)	81.8(1)	O(5)–Mn(4)–O(3)	79.4(1)
O(11)–Mn(2)–N(2)	89.6(1)	O(13)–Mn(4)–N(8)	88.4(2)
O(5)–Mn(2)–N(2)	147.0(1)	O(5)–Mn(4)–N(8)	109.8(1)
O(7)–Mn(2)–N(2)	108.4(1)	O(3)–Mn(4)–N(8)	143.2(1)
O(11)–Mn(2)–N(6)	98.4(1)	O(13)–Mn(4)–N(4)	90.4(2)
O(5)–Mn(2)–N(6)	73.1(1)	O(5)–Mn(4)–N(4)	151.2(1)
O(7)–Mn(2)–N(6)	154.8(1)	O(3)–Mn(4)–N(4)	71.8(1)
N(2)–Mn(2)–N(6)	94.6(1)	N(8)–Mn(4)–N(4)	94.1(1)
O(11)–Mn(2)–O(1)	154.8(1)	O(13)–Mn(4)–O(7)	158.3(1)
O(5)–Mn(2)–O(1)	80.2(1)	O(5)–Mn(4)–O(7)	78.2(1)
O(7)–Mn(2)–O(1)	78.5(1)	O(3)–Mn(4)–O(7)	77.2(1)
N(2)–Mn(2)–O(1)	71.7(1)	N(8)–Mn(4)–O(7)	70.5(1)
N(6)–Mn(2)–O(1)	99.8(1)	N(4)–Mn(4)–O(7)	95.8(1)

**Fig. 3** Perspective view of the cubane cores in **2** (a) and **3** (b).

and four oxygen atoms each from a dpd–H ligand and each at alternating corners, where each Zn(II) atom is coordinated in a distorted octahedral geometry by two nitrogen atoms each from a dpd–H ligand and four oxygen atoms. Besides three

$\mu_3$ -alkoxo oxygen atoms each from a dpd–H ligand, the fourth oxygen atom is from a monodentate acetate group for the Zn(1) and Zn(2) atoms, and is from an aqua ligand for the Zn(3) and Zn(4) atoms (Fig. 4(a)). Another oxygen atom of each dpd–H ligand also remains protonated and unbound to metal ions, similar to those in **1–3**.

It should be noted that there are only two reported zinc(II) complexes [ $\text{Zn}_4(\text{HL})_4 \cdot 4\text{MeCN}$ ] [HL = divalent bis(benzoylacetone)-1,3-diiiminopropan-2-ol] and [ $\text{Zn}_4(\text{L}_2)_4 \cdot 4\cdot 5\text{H}_2\text{O}$ ] [ $\text{H}_2\text{L}_2 = 3\text{-}[N\text{-}(\text{2-pyridylmethyl})\text{iminomethyl}]$ salicylic acid] that contain  $\text{Zn}_4\text{O}_4$  cubane cores besides this work.<sup>7</sup> The zinc atoms in **4** are in a slightly distorted octahedral coordination geometry. In contrast, both zinc and oxygen atoms in common organometallic  $[\text{RZn}(\text{OR}')_4]$  cubanes<sup>20</sup> possess highly distorted tetrahedral geometry, and the external angles are accordingly larger than those within the cube. The  $\text{Zn} \cdots \text{Zn}$  separations in **4** are 3.221–3.328 Å, which is comparable to those found in related  $\text{Zn}_4\text{O}_4$  cubane-like complexes.<sup>7</sup>

Each cubane core in **5** is similar to that in **4**, which also contains a cubane  $\text{M}_4\text{O}_4$  core (Fig. 4(b)), perchlorate anions and lattice water molecules. A minor structural difference in **5** lies in the seven-coordination geometry of the Cd(4) atom, which is bidentately chelated by an acetate group [ $\text{Cd}–\text{O}$  2.374(8) and 2.569(8) Å]. It is interesting that **5** is the first cadmium(II) complex containing  $\text{Cd}_4\text{O}_4$  core except the organometallic  $[\text{RCd}(\text{OR}')_4]$  cubanes to date.<sup>20</sup>

The structure of **6** also contains similar cubane-type  $[\text{Ni}_4(\text{dpd}-\text{H})_4]$  species (Fig. 5, Table 7), perchlorate anions and lattice water molecules, but the cubane core is different from those in **1–5**. The Ni(1) and Ni(2) atoms are connected by a

**Table 4** Selected interatomic contacts ( $\text{\AA}$ ) and bond angles ( $^\circ$ ) for **3**

Co(1)–O(1)	2.029(3)	Co(3)–O(5)	1.998(3)
Co(1)–O(11)	2.047(3)	Co(3)–O(21)	2.046(3)
Co(1)–N(31)	2.103(3)	Co(3)–N(42)	2.105(3)
Co(1)–O(21)	2.126(2)	Co(3)–O(31)	2.118(2)
Co(1)–N(11)	2.185(3)	Co(3)–N(21)	2.173(3)
Co(1)–O(31)	2.252(3)	Co(3)–O(41)	2.237(3)
Co(2)–O(31)	2.030(3)	Co(4)–O(41)	2.044(2)
Co(2)–O(3)	2.062(3)	Co(4)–O(1w)	2.108(3)
Co(2)–O(41)	2.107(2)	Co(4)–N(41)	2.129(3)
Co(2)–N(12)	2.109(3)	Co(4)–O(11)	2.134(2)
Co(2)–N(32)	2.145(3)	Co(4)–N(22)	2.140(3)
Co(2)–O(11)	2.227(3)	Co(4)–O(21)	2.161(3)
O(1)–Co(1)–O(11)	112.9(1)	O(5)–Co(3)–O(21)	112.8(1)
O(1)–Co(1)–N(31)	94.8(1)	O(5)–Co(3)–N(42)	95.4(1)
O(11)–Co(1)–N(31)	149.9(1)	O(21)–Co(3)–N(42)	149.6(1)
O(1)–Co(1)–O(21)	97.9(1)	O(5)–Co(3)–O(31)	96.9(1)
O(11)–Co(1)–O(21)	81.4(1)	O(21)–Co(3)–O(31)	81.6(1)
N(31)–Co(1)–O(21)	107.2(1)	N(42)–Co(3)–O(31)	107.0(1)
O(1)–Co(1)–N(11)	88.4(1)	O(5)–Co(3)–N(21)	91.2(1)
O(11)–Co(1)–N(11)	76.1(1)	O(21)–Co(3)–N(21)	76.3(1)
N(31)–Co(1)–N(11)	94.0(1)	N(42)–Co(3)–N(21)	92.6(1)
O(21)–Co(1)–N(11)	157.2(1)	O(31)–Co(3)–N(21)	157.9(1)
O(1)–Co(1)–O(31)	165.6(1)	O(5)–Co(3)–O(41)	165.7(1)
O(11)–Co(1)–O(31)	79.9(1)	O(21)–Co(3)–O(41)	79.7(1)
N(31)–Co(1)–O(31)	74.4(1)	N(42)–Co(3)–O(41)	74.1(1)
O(21)–Co(1)–O(31)	76.8(1)	O(31)–Co(3)–O(41)	77.5(1)
N(11)–Co(1)–O(31)	101.7(1)	N(21)–Co(3)–O(41)	98.9(1)
O(31)–Co(2)–O(3)	116.5(1)	O(41)–Co(4)–O(1w)	111.8(1)
O(31)–Co(2)–O(41)	82.5(1)	O(41)–Co(4)–N(41)	77.2(1)
O(3)–Co(2)–O(41)	91.6(1)	O(1w)–Co(4)–N(41)	89.6(1)
O(31)–Co(2)–N(12)	151.0(1)	O(41)–Co(4)–O(11)	80.5(1)
O(3)–Co(2)–N(12)	91.2(1)	O(1w)–Co(4)–O(11)	89.5(1)
O(41)–Co(2)–N(12)	106.4(1)	N(41)–Co(4)–O(11)	155.5(1)
O(31)–Co(2)–N(32)	77.0(1)	O(41)–Co(4)–N(22)	153.5(1)
O(3)–Co(2)–N(32)	95.5(1)	O(1w)–Co(4)–N(22)	93.9(1)
O(41)–Co(2)–N(32)	159.3(1)	N(41)–Co(4)–N(22)	97.4(1)
N(12)–Co(2)–N(32)	92.9(1)	O(11)–Co(4)–N(22)	107.1(1)
O(31)–Co(2)–O(11)	80.9(1)	O(41)–Co(4)–O(21)	81.5(1)
O(3)–Co(2)–O(11)	158.2(1)	O(1w)–Co(4)–O(21)	160.6(1)
O(41)–Co(2)–O(11)	77.0(1)	N(41)–Co(4)–O(21)	107.6(1)
N(12)–Co(2)–O(11)	74.7(1)	O(11)–Co(4)–O(21)	78.6(1)
N(32)–Co(2)–O(11)	101.6(1)	N(22)–Co(4)–O(21)	75.4(1)

$\mu\text{-O}_2\text{CMe}$  bridge with a separation of 2.944(2)  $\text{\AA}$ , and further ligated by a nitrogen atom from a dpd – H ligand, three oxygen atoms from different dpd – H ligands and a monodentate acetate ion; while the Ni(3) and Ni(4) atoms with a separation of 3.019(2)  $\text{\AA}$  are coordinated by three nitrogen atoms and three oxygen atoms from different dpd – H ligands. The other four Ni  $\cdots$  Ni separations are 3.168(2), 3.233(2), 3.192(2) and 3.241(2)  $\text{\AA}$ .

It has been reported that there are only three cubane-like nickel(II) complexes containing dinuclear  $\text{Ni}_2(\mu\text{-O}_2\text{CMe})$  subunits similar to **6**.<sup>21</sup> However, the former contain two  $\text{Ni}_2(\mu\text{-O}_2\text{CMe})$  subunits while the latter contains only one  $\text{Ni}_2(\mu\text{-O}_2\text{CMe})$  subunit.

### Magnetic properties

Magnetic susceptibility data were measured with polycrystalline samples of **2**, **3** and **6** in a 5.0 kG field over the temperature range 4–298 K. Figs. 6–8 shows the effective magnetic moments per  $\text{M}_4$  unit ( $\mu_{\text{eff}}$ ) versus temperature. For **2**, the effective moment of 10.95  $\mu_{\text{B}}$  per  $\text{Mn}_4$  unit at 298 K is below the value ( $(\sum 4S_i(S_i + 1))^{1/2} = 11.83 \mu_{\text{B}}$ ) for a non-interacting  $\text{Mn}_4$  unit. On lowering the temperature, the magnetic moment decreases slowly from 10.95  $\mu_{\text{B}}$  at 298 K to 10.03  $\mu_{\text{B}}$  at 18.4 K, then decreases dramatically to ca. 3.96  $\mu_{\text{B}}$  at 2.0 K, indicating an intramolecular antiferromagnetic interaction. For **3**, the effective moment at 298 K is 5.02  $\mu_{\text{B}}$  for per  $\text{Co}_4$  unit, and **6**, and the effective moment at 282 K is 5.51  $\mu_{\text{B}}$  for per  $\text{Ni}_4$  unit. On lowering the temperature, the magnetic moments increase slowly from 5.02  $\mu_{\text{B}}$  at 298 K to 6.43  $\mu_{\text{B}}$  at 9.1 K for **3**, and from 5.51  $\mu_{\text{B}}$

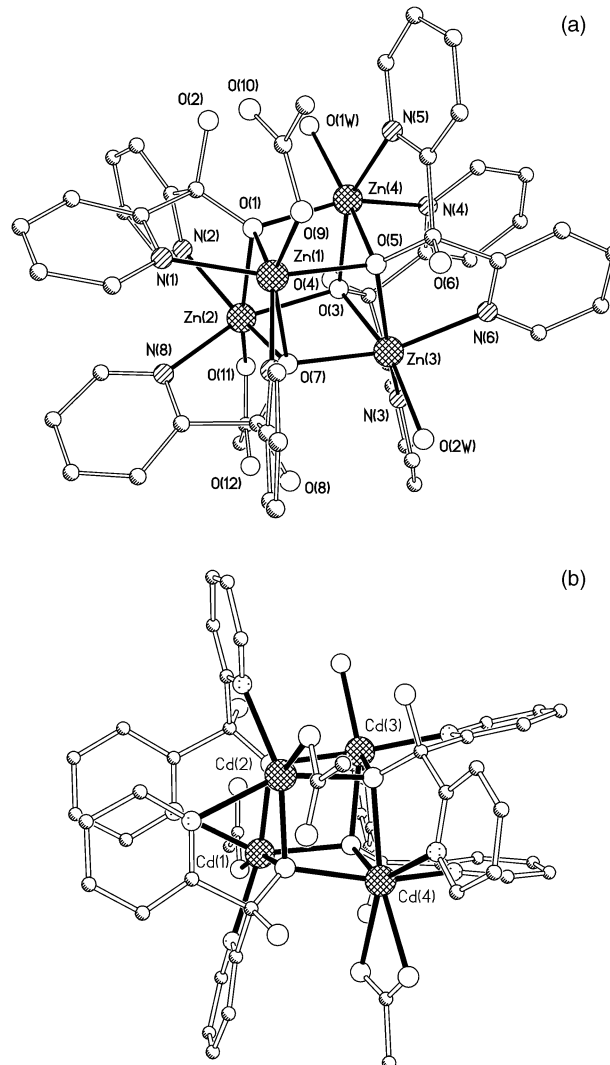
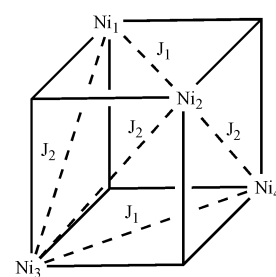


Fig. 4 Perspective view of the cubane cores in **4** (a) and **5** (b).

at 282 K to 6.61  $\mu_{\text{B}}$  at 30 K for **6**, then decreases to ca. 6.09  $\mu_{\text{B}}$  at 4.4 K for **3** and to 3.99  $\mu_{\text{B}}$  at 4.5 K for **6**, indicating weak intramolecular ferromagnetic interactions. Since the tetranuclear units are isolated in the three compounds, the intermolecular interactions are expected to be negligible.

For **2**, we assure that all the coupling values between Mn(II) atoms are equal in an ideal cube geometry, therefore, the experimental data can be fitted using the expression derived from the isotropic Heisenberg Hamiltonian ( $H = -2J(S_1S_2 + S_1S_3 + S_1S_4 + S_2S_3 + S_2S_4 + S_3S_4)$ ). The best fit parameters are found to be  $J = -0.61 \text{ cm}^{-1}$ ,  $g = 1.98$  with a reliability factor  $R = 6.1 \times 10^{-4}$  ( $R = \sum (\chi_{\text{obs}} - \chi_{\text{calc}})^2 / \sum (\chi_{\text{obs}})^2$ ).

For **6**, in order to estimate the intracluster exchange, a lower symmetry model with two different coupling constant values,  $J_1$  and  $J_2$ , are adopted. The corresponding network of exchange pathways is shown in Scheme 1. The experimental data can



Scheme 1

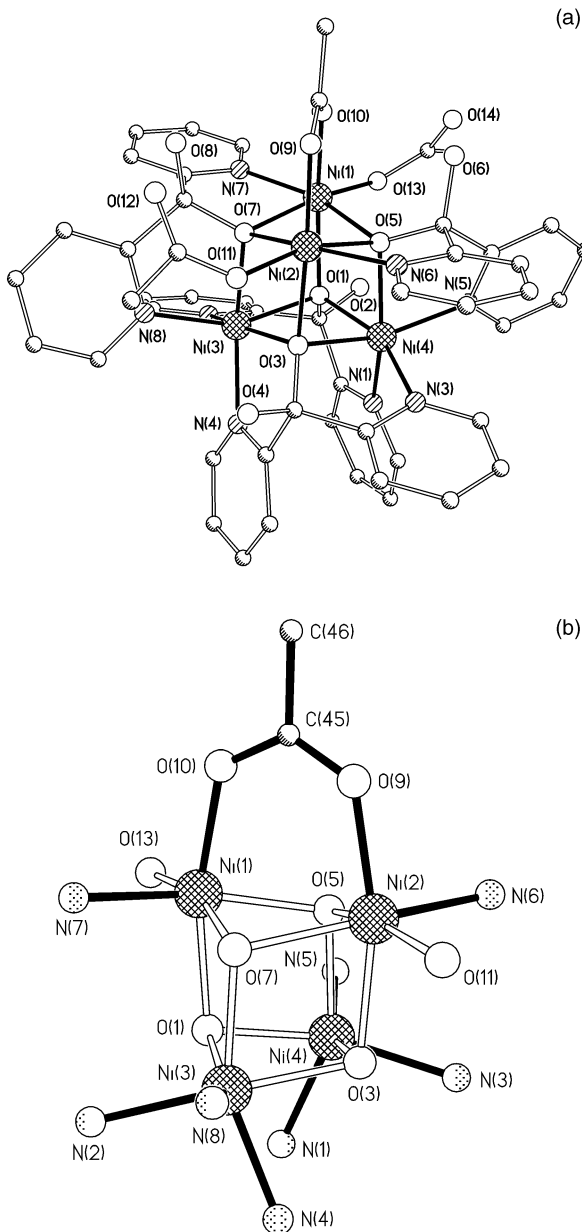


**Fig. 5** Perspective view of the cubane core (a) and bridging skeleton of the four Ni(II) atoms in the cubane core (b) in **6**.

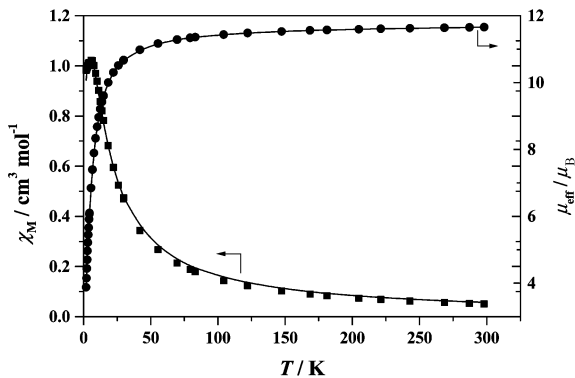


**Fig. 6** Plot of effective magnetic moment ( $\mu_{\text{eff}}$ ) per  $\text{Mn}^{\text{II}}_4$  vs.  $T$  for **2**.

be fitted using the expression derived from the Heisenberg Hamiltonian ( $H = -2J_1(S_1S_2 + S_3S_4) - 2J_2(S_1S_3 + S_1S_4 + S_2S_3 + S_2S_4)$ ), similar to the methods reported previously.<sup>22</sup> The best fit parameters are found to be  $J_1 = 6.04 \text{ cm}^{-1}$ ,  $J_2 = -1.47 \text{ cm}^{-1}$ , and  $g = 2.12$ ,  $R = 1.01 \times 10^{-5}$ .

**Table 5** Selected interatomic contacts (Å) and bond angles (°) for **4**

Zn(1)–O(9)	2.022(5)	Zn(3)–O(7)	2.074(4)
Zn(1)–O(1)	2.078(5)	Zn(3)–O(5)	2.088(5)
Zn(1)–N(7)	2.100(6)	Zn(3)–N(3)	2.088(6)
Zn(1)–N(1)	2.117(6)	Zn(3)–O(2w)	2.099(5)
Zn(1)–O(5)	2.142(5)	Zn(3)–N(6)	2.125(6)
Zn(1)–O(7)	2.264(5)	Zn(3)–O(3)	2.224(5)
Zn(2)–O(11)	2.040(5)	Zn(4)–O(3)	2.072(4)
Zn(2)–O(7)	2.068(4)	Zn(4)–N(5)	2.081(6)
Zn(2)–N(2)	2.096(6)	Zn(4)–O(1w)	2.100(5)
Zn(2)–N(8)	2.116(6)	Zn(4)–O(1)	2.115(5)
Zn(2)–O(3)	2.139(5)	Zn(4)–N(4)	2.133(6)
Zn(2)–O(1)	2.220(4)	Zn(4)–O(5)	2.216(5)
O(9)–Zn(1)–O(1)	117.3(2)	O(7)–Zn(3)–O(5)	80.3(2)
O(9)–Zn(1)–N(7)	91.8(2)	O(7)–Zn(3)–N(3)	105.9(2)
O(1)–Zn(1)–N(7)	150.6(2)	O(5)–Zn(3)–N(3)	153.4(2)
O(9)–Zn(1)–N(1)	98.4(2)	O(7)–Zn(3)–O(2w)	94.7(2)
O(1)–Zn(1)–N(1)	76.0(2)	O(5)–Zn(3)–O(2w)	113.8(2)
N(7)–Zn(1)–N(1)	96.4(2)	N(3)–Zn(3)–O(2w)	91.7(2)
O(9)–Zn(1)–O(5)	88.1(2)	O(7)–Zn(3)–N(6)	154.4(2)
O(1)–Zn(1)–O(5)	80.0(2)	O(5)–Zn(3)–N(6)	75.5(2)
N(7)–Zn(1)–O(5)	107.1(2)	N(3)–Zn(3)–N(6)	99.5(2)
N(1)–Zn(1)–O(5)	155.4(2)	O(2w)–Zn(3)–N(6)	87.7(2)
O(9)–Zn(1)–O(7)	153.6(2)	O(7)–Zn(3)–O(3)	78.1(2)
O(1)–Zn(1)–O(7)	80.1(2)	O(5)–Zn(3)–O(3)	81.3(2)
N(7)–Zn(1)–O(7)	74.6(2)	N(3)–Zn(3)–O(3)	75.0(2)
N(1)–Zn(1)–O(7)	105.4(2)	O(2w)–Zn(3)–O(3)	162.3(2)
O(5)–Zn(1)–O(7)	75.0(2)	N(6)–Zn(3)–O(3)	105.8(2)
O(11)–Zn(2)–O(7)	115.2(2)	O(3)–Zn(4)–N(5)	153.2(2)
O(11)–Zn(2)–N(2)	91.5(2)	O(3)–Zn(4)–O(1w)	112.7(2)
O(7)–Zn(2)–N(2)	152.7(2)	N(5)–Zn(4)–O(1w)	92.5(2)
O(11)–Zn(2)–N(8)	97.1(2)	O(3)–Zn(4)–O(1)	80.4(2)
O(7)–Zn(2)–N(8)	76.2(2)	N(5)–Zn(4)–O(1)	108.4(2)
N(2)–Zn(2)–N(8)	96.1(2)	O(1w)–Zn(4)–O(1)	93.1(2)
O(11)–Zn(2)–O(3)	87.9(2)	O(3)–Zn(4)–N(4)	75.6(2)
O(7)–Zn(2)–O(3)	80.2(2)	N(5)–Zn(4)–N(4)	95.9(2)
N(2)–Zn(2)–O(3)	107.4(2)	O(1w)–Zn(4)–N(4)	90.4(2)
N(8)–Zn(2)–O(3)	155.8(2)	O(1)–Zn(4)–N(4)	155.2(2)
O(11)–Zn(2)–O(1)	155.4(2)	O(3)–Zn(4)–O(5)	81.8(2)
O(7)–Zn(2)–O(1)	81.4(2)	N(5)–Zn(4)–O(5)	75.8(2)
N(2)–Zn(2)–O(1)	75.3(2)	O(1w)–Zn(4)–O(5)	161.5(2)
N(8)–Zn(2)–O(1)	104.9(2)	O(1)–Zn(4)–O(5)	77.5(2)
O(3)–Zn(2)–O(1)	76.6(2)	N(4)–Zn(4)–O(5)	104.9(2)

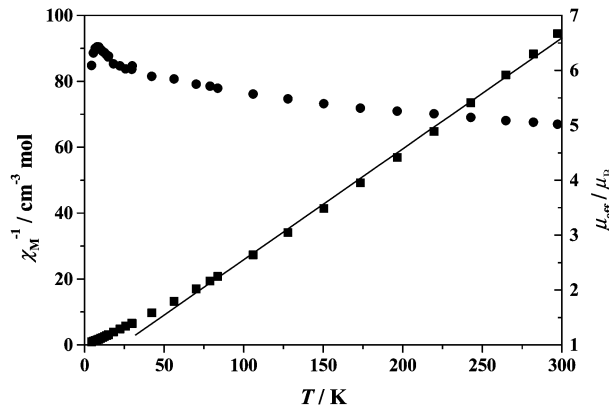


**Fig. 7** Plot of effective magnetic moment ( $\mu_{\text{eff}}$ ) per  $\text{Co}^{\text{II}}_4$  vs.  $T$  for **3**.

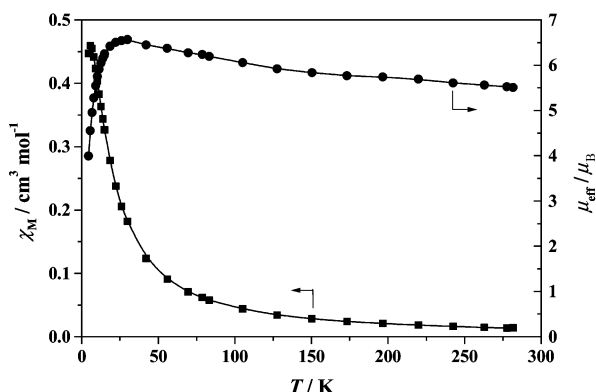
While for **3**, it is not possible to fit the behavior of an array of four orbitally degenerate Co(II) centers given current theory,<sup>8d,e</sup> the Curie–Weiss law ( $\chi_M = C/(T - \theta)$ ) is obeyed down to 50 K with  $C = 2.97 \text{ K cm}^3 \text{ mol}^{-1}$  and  $\theta = 23.05 \text{ K}$ , indicating an intramolecular ferromagnetic interaction in **3**, which is similar to that found in a recently reported Co(II) cluster.<sup>8e</sup>

#### Luminescent properties of complexes **4** and **5**

Crystals of both **4** and **5** are luminescent at both ambient and cryogenic temperatures. Upon excitation at 325 nm, **4** and **5** display similar intense blue photoluminescence in the solid state

**Table 6** Selected interatomic contacts ( $\text{\AA}$ ) and bond angles ( $^\circ$ ) for **5**

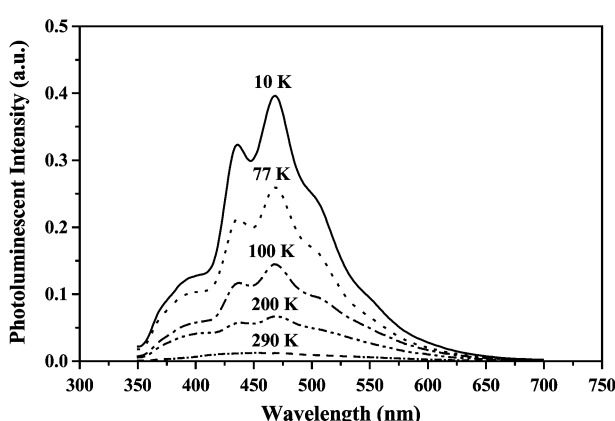
Cd(1)–O(9)	2.187(6)	Cd(3)–O(1)	2.266(5)
Cd(1)–O(7)	2.243(5)	Cd(3)–O(5)	2.286(4)
Cd(1)–O(1)	2.306(5)	Cd(3)–O(7)	2.303(5)
Cd(1)–N(3)	2.316(6)	Cd(3)–O(1w)	2.308(6)
Cd(1)–N(1)	2.337(6)	Cd(3)–N(7)	2.320(6)
Cd(1)–O(3)	2.404(5)	Cd(4)–O(3)	2.254(5)
Cd(2)–O(5)	2.263(5)	Cd(4)–N(6)	2.283(7)
Cd(2)–O(3)	2.276(5)	Cd(4)–N(8)	2.350(7)
Cd(2)–O(11)	2.283(6)	Cd(4)–O(7)	2.356(5)
Cd(2)–N(4)	2.311(7)	Cd(4)–O(14)	2.374(8)
Cd(2)–N(2)	2.318(7)	Cd(4)–O(5)	2.433(5)
Cd(2)–O(1)	2.391(4)	Cd(4)–O(13)	2.569(8)
Cd(3)–N(5)	2.258(7)		
O(9)–Cd(1)–O(7)	104.1(2)	N(5)–Cd(3)–O(7)	107.0(2)
O(9)–Cd(1)–O(1)	121.4(2)	O(1)–Cd(3)–O(7)	78.2(2)
O(7)–Cd(1)–O(1)	78.6(2)	O(5)–Cd(3)–O(7)	79.1(2)
O(9)–Cd(1)–N(3)	93.5(2)	N(5)–Cd(3)–O(1w)	94.0(2)
O(7)–Cd(1)–N(3)	112.1(2)	O(1)–Cd(3)–O(1w)	90.0(2)
O(1)–Cd(1)–N(3)	140.7(2)	O(5)–Cd(3)–O(1w)	120.1(2)
O(9)–Cd(1)–N(1)	91.9(2)	O(7)–Cd(3)–O(1w)	155.6(2)
O(7)–Cd(1)–N(1)	147.4(2)	N(5)–Cd(3)–N(7)	102.3(2)
O(1)–Cd(1)–N(1)	68.8(2)	O(1)–Cd(3)–N(7)	107.7(2)
N(3)–Cd(1)–N(1)	94.8(2)	O(5)–Cd(3)–N(7)	146.4(2)
O(9)–Cd(1)–O(3)	161.5(2)	O(7)–Cd(3)–N(7)	70.8(2)
O(7)–Cd(1)–O(3)	76.7(2)	O(1w)–Cd(3)–N(7)	93.1(2)
O(1)–Cd(1)–O(3)	77.1(2)	O(3)–Cd(4)–N(6)	111.8(2)
N(3)–Cd(1)–O(3)	69.6(2)	O(3)–Cd(4)–N(8)	145.7(2)
N(1)–Cd(1)–O(3)	96.9(2)	N(6)–Cd(4)–N(8)	94.5(2)
O(5)–Cd(2)–O(3)	80.2(2)	O(3)–Cd(4)–O(7)	77.5(2)
O(5)–Cd(2)–O(11)	92.0(2)	N(6)–Cd(4)–O(7)	139.2(2)
O(3)–Cd(2)–O(11)	128.7(2)	N(8)–Cd(4)–O(7)	68.2(2)
O(5)–Cd(2)–N(4)	151.2(2)	O(3)–Cd(4)–O(14)	110.8(2)
O(3)–Cd(2)–N(4)	71.0(2)	N(6)–Cd(4)–O(14)	84.8(2)
O(11)–Cd(2)–N(4)	104.4(2)	N(8)–Cd(4)–O(14)	92.5(3)
O(5)–Cd(2)–N(2)	108.7(2)	O(7)–Cd(4)–O(14)	130.7(2)
O(3)–Cd(2)–N(2)	143.3(2)	O(3)–Cd(4)–O(5)	77.1(2)
O(11)–Cd(2)–N(2)	87.3(2)	N(6)–Cd(4)–O(5)	69.0(2)
N(4)–Cd(2)–N(2)	95.8(2)	N(8)–Cd(4)–O(5)	93.3(2)
O(5)–Cd(2)–O(1)	77.6(2)	O(7)–Cd(4)–O(5)	75.2(2)
O(3)–Cd(2)–O(1)	77.9(2)	O(14)–Cd(4)–O(5)	153.5(2)
O(11)–Cd(2)–O(1)	149.9(2)	O(3)–Cd(4)–O(13)	90.3(2)
N(4)–Cd(2)–O(1)	97.6(2)	N(6)–Cd(4)–O(13)	136.3(2)
N(2)–Cd(2)–O(1)	70.0(2)	N(8)–Cd(4)–O(13)	84.8(2)
N(5)–Cd(3)–O(1)	149.5(2)	O(7)–Cd(4)–O(13)	80.8(2)
N(5)–Cd(3)–O(5)	72.1(2)	O(14)–Cd(4)–O(13)	51.7(2)
O(1)–Cd(3)–O(5)	79.8(2)	O(5)–Cd(4)–O(13)	154.7(2)

Fig. 8 Plot of effective magnetic moment ( $\mu_{\text{eff}}$ ) per  $\text{Ni}^{\text{II}}_4$  vs.  $T$  for **6**.

with two emission maxima at *ca.* 430 and 475 nm, which are much more well resolved at low temperature (Fig. 9). From 290 to 10 K, a continuing increase in emission intensity is observed, while the emission energy and band shape remain constant. The dpk ligand has no emission in the visible region. When it is bound to a zinc or cadmium center, blue luminescence was observed. Because  $\text{Zn(O}_2\text{CMe)}_2$  and  $\text{Cd(O}_2\text{CMe)}_2$  are also not luminescent, the observed luminescence of the complexes is attributed to the coordination of dpd – H ligands. In the crystal structures of **4** and **5**, there are intramolecular  $\pi$ – $\pi$  stacking

**Table 7** Selected interatomic contacts ( $\text{\AA}$ ) and bond angles ( $^\circ$ ) for **6**

Ni(1)–O(13)	2.003(5)	Ni(3)–O(3)	2.016(4)
Ni(1)–O(10)	2.003(5)	Ni(3)–N(8)	2.030(5)
Ni(1)–O(7)	2.019(4)	Ni(3)–N(4)	2.047(5)
Ni(1)–N(7)	2.056(6)	Ni(3)–O(7)	2.067(4)
Ni(1)–O(5)	2.071(4)	Ni(3)–N(2)	2.073(5)
Ni(1)–O(1)	2.165(4)	Ni(3)–O(1)	2.094(4)
Ni(1)–Ni(2)	2.944(1)	Ni(4)–O(1)	2.011(4)
Ni(2)–O(9)	2.001(5)	Ni(4)–N(5)	2.012(6)
Ni(2)–O(11)	2.014(5)	Ni(4)–N(3)	2.056(5)
Ni(2)–O(5)	2.023(4)	Ni(4)–N(1)	2.059(5)
Ni(2)–N(6)	2.068(5)	Ni(4)–O(5)	2.067(4)
Ni(2)–O(7)	2.072(4)	Ni(4)–O(3)	2.103(4)
Ni(2)–O(3)	2.158(4)		
O(13)–Ni(1)–O(10)	100.5(2)	O(3)–Ni(3)–N(8)	106.7(2)
O(13)–Ni(1)–O(7)	165.0(2)	O(3)–Ni(3)–N(4)	78.3(2)
O(10)–Ni(1)–O(7)	93.4(2)	N(8)–Ni(3)–N(4)	98.1(2)
O(13)–Ni(1)–N(7)	95.6(2)	O(3)–Ni(3)–O(7)	79.2(2)
O(10)–Ni(1)–N(7)	91.7(2)	N(8)–Ni(3)–O(7)	78.5(2)
O(7)–Ni(1)–N(7)	78.2(2)	N(4)–Ni(3)–O(7)	155.1(2)
O(13)–Ni(1)–O(5)	100.6(2)	O(3)–Ni(3)–N(2)	158.2(2)
O(10)–Ni(1)–O(5)	91.4(2)	N(8)–Ni(3)–N(2)	94.9(2)
O(7)–Ni(1)–O(5)	84.6(2)	N(4)–Ni(3)–N(2)	96.4(2)
N(7)–Ni(1)–O(5)	162.6(2)	O(7)–Ni(3)–N(2)	108.5(2)
O(13)–Ni(1)–O(1)	87.2(2)	O(3)–Ni(3)–O(1)	83.7(2)
O(10)–Ni(1)–O(1)	166.5(2)	N(8)–Ni(3)–O(1)	154.6(2)
O(7)–Ni(1)–O(1)	80.4(2)	N(4)–Ni(3)–O(1)	106.8(2)
N(7)–Ni(1)–O(1)	98.6(2)	O(7)–Ni(3)–O(1)	81.0(2)
O(5)–Ni(1)–O(1)	76.1(2)	N(2)–Ni(3)–O(1)	77.6(2)
O(9)–Ni(2)–O(11)	100.6(2)	O(1)–Ni(4)–N(5)	105.8(2)
O(9)–Ni(2)–O(5)	93.2(2)	O(1)–Ni(4)–N(3)	157.4(2)
O(11)–Ni(2)–O(5)	164.8(2)	N(5)–Ni(4)–N(3)	96.7(2)
O(9)–Ni(2)–N(6)	92.2(2)	O(1)–Ni(4)–N(1)	78.5(2)
O(11)–Ni(2)–N(6)	95.5(2)	N(5)–Ni(4)–N(1)	97.1(2)
O(5)–Ni(2)–N(6)	77.7(2)	N(3)–Ni(4)–N(1)	96.3(2)
O(9)–Ni(2)–O(7)	91.9(2)	O(1)–Ni(4)–O(5)	79.7(2)
O(11)–Ni(2)–O(7)	101.0(2)	N(5)–Ni(4)–O(5)	78.4(2)
O(5)–Ni(2)–O(7)	84.5(2)	N(3)–Ni(4)–O(5)	108.1(2)
N(6)–Ni(2)–O(7)	161.9(2)	N(1)–Ni(4)–O(5)	155.5(2)
O(9)–Ni(2)–O(3)	166.3(2)	O(1)–Ni(4)–O(3)	83.6(2)
O(11)–Ni(2)–O(3)	88.0(2)	N(5)–Ni(4)–O(3)	154.3(2)
O(5)–Ni(2)–O(3)	79.6(2)	N(3)–Ni(4)–O(3)	77.2(2)
N(6)–Ni(2)–O(3)	97.6(2)	N(1)–Ni(4)–O(3)	108.4(2)
O(7)–Ni(2)–O(3)	75.9(2)	O(5)–Ni(4)–O(3)	79.9(2)
Ni(1)–O(7)–Ni(2)	92.0(2)	Ni(4)–O(1)–Ni(1)	101.4(2)
Ni(2)–O(5)–Ni(1)	91.9(2)	Ni(3)–O(3)–Ni(2)	101.8(2)
Ni(4)–O(1)–Ni(3)	94.7(2)	Ni(2)–O(5)–Ni(4)	102.6(2)
Ni(3)–O(1)–Ni(1)	96.1(2)	Ni(4)–O(5)–Ni(1)	102.7(2)
Ni(3)–O(3)–Ni(4)	94.2(2)	Ni(1)–O(7)–Ni(3)	101.6(2)
Ni(4)–O(3)–Ni(2)	97.0(2)	Ni(3)–O(7)–Ni(2)	103.1(2)

Fig. 9 Solid state photo-induced emission spectra of **4** at ambient and cryogenic temperatures with  $\lambda_{\text{ex}} = 325 \text{ nm}$ .

interactions between the pyridyl rings of adjacent dpd – H ligands, with the shortest atomic separation distances being 3.7–3.9 Å. This phenomenon are very similar to those found in the previously reported Zn(II) complexes with polypyridyl ligands,<sup>23–25</sup> the blue luminescence of the complexes may be,

therefore, ascribed to a  $\pi^* \rightarrow \pi$  transition of the dpd-H ligand. The results reported here along with those<sup>26</sup> reported previously suggest that these Zn(II) and Cd(II) metal-organic compounds are potential luminescent materials exhibiting blue and/or white emissions.

## Conclusions

Six cubane-type complexes comprising similar  $[M_4O_4]^{n+}$  cores [ $M = Mn(II)$ ,  $Co(II)$ ,  $Ni(II)$ ,  $Zn(II)$  and  $Cd(II)$ ] have been synthesised in a facile route utilizing the *gem*-diol form of di-2-pyridyl ketone as a ligand. X-Ray structural analyses show the four metal ions and  $\mu_3$ -bridging alkoxo oxygen atoms are located at alternating vertices of a cube, with either pyridyl, acetate or aqua groups on the exterior of the core. Magnetic studies indicate the presence of an antiferromagnetic behavior in **2** and ferromagnetic behavior in **3** and **6**. The temperature dependence of the magnetic susceptibility for **6** was fitted with  $J_1 = 6.04 \text{ cm}^{-1}$ ,  $J_2 = -1.47 \text{ cm}^{-1}$ , and  $g = 2.12$ . The difference in sign between the  $J_1$  and  $J_2$  superexchange interactions is in good agreement with the different types of faces present in this  $Ni_4O_4$  cubane core. Both **4** and **5** show similar ambient and cryogenic temperature emissions in the solid state.

## Acknowledgements

This work was supported by the NSFC (No. 20001008, 29971033), the Ministry of Education of China and Zhongshan University.

## References

- R. H. Holm, S. Ciurli and J. A. Weigel, *Prog. Inorg. Chem.*, 1990, **38**, 1; D. Sellmann, *Angew. Chem., Int. Ed. Engl.*, 1993, **32**, 64; W. F. Ruettinger, D. M. Ho and G. C. Dismukes, *Inorg. Chem.*, 1999, **38**, 1037 and references therein.
- Magnetic Molecular Materials*, ed. D. Gatteschi, O. Kahn and F. Palacio, Kluwer Academic Publishers, Dordrecht, The Netherlands, 1991, NATO ASI Series E, vol. 198; S. M. J. Aubin, N. R. Dilley, L. Pardi, J. Krzystek, M. W. Wemple, L.-C. Brunel, M. B. Maple, G. Christou and D. N. Hendrickson, *J. Am. Chem. Soc.*, 1998, **120**, 4991; R. G. Raptis, I. P. Georgakaki and D. C. R. Hockless, *Angew. Chem., Int. Ed.*, 1999, **38**, 1634; K. Dimitrou, A. D. Brown, K. Folting and G. Christou, *Inorg. Chem.*, 1999, **38**, 1834 and references therein.
- S.-W. Lai, K.-K. Cheung, M. C.-W. Chan and C.-M. Che, *Angew. Chem., Int. Ed.*, 1998, **37**, 182; Y. Ma, H.-Y. Chao, Y. Wu, S. T. Lee, W.-Y. Yu and C.-M. Che, *Chem. Commun.*, 1998, 2491.
- K. Isobe and A. Yagasaki, *Acc. Chem. Res.*, 1993, **26**, 524.
- (a) K. Dimitrou, K. Folting, W. E. Streib and G. Christou, *J. Am. Chem. Soc.*, 1993, **115**, 6432; (b) K. L. Taft, A. Caneschi, L. E. Pence, C. D. Delfs, G. C. Papaefthymiou and S. J. Lippard, *J. Am. Chem. Soc.*, 1993, **115**, 11753 and references therein.
- M.-L. Tong, H. K. Lee, S.-L. Zheng and X.-M. Chen, *Chem. Lett.*, 1999, 1087.
- M. Mikuriya, *Inorg. Chem. Commun.*, 2000, **3**, 227; A. Erxleben, *Inorg. Chem.*, 2001, **40**, 208.
- (a) V. Tangoulis, S. Paschalidou, E. G. Bakalbassis, S. P. Perlepes, C. P. Raptopoulou and A. Terzis, *Chem. Commun.*, 1996, 1297; (b) V. Tangoulis, C. P. Raptopoulou, S. Paschalidou, E. G. Bakalbassis, S. P. Perlepes and A. Terzis, *Angew. Chem., Int. Ed. Engl.*, 1997, **36**, 1083; (c) V. Tangoulis, C. P. Raptopoulou, S. Paschalidou, A. E. Tsohos, E. G. Bakalbassis, A. Terzis and S. P. Perlepes, *Inorg. Chem.*, 1997, **36**, 5270; (d) A. Tsohos, S. Dionyssopoulou, C. P. Raptopoulou, A. Terzis, E. G. Bakalbassis and S. P. Perlepes, *Angew. Chem., Int. Ed.*, 1999, **38**, 983; (e) G. S. Papaefstathiou, S. P. Perlepes, A. Escuer, R. Vicente, M. Font-Bardia and X. Solans, *Angew. Chem., Int. Ed.*, 2001, **40**, 884.
- S. R. Breeze, S. Wang, J. E. Greedan and N. P. Raju, *Inorg. Chem.*, 1996, **35**, 6944; Z. Serna, M. G. Barandika, R. Cortés, M. K. Urtiaga, G. E. Barberis and T. Rojo, *J. Chem. Soc., Dalton Trans.*, 2000, **39**; M. G. Barandika, Z. Serna, R. Cortés, L. Lezama, K. Urtiaga, M. I. Arriortua and T. Rojo, *Chem. Commun.*, 2001, 45; Z. E. Serna, L. Lezama, M. K. Urtiaga, M. I. Arriortua, M. G. Barandika, R. Cortés and T. Rojo, *Angew. Chem., Int. Ed.*, 2000, **39**, 344; Z. E. Serna, M. K. Urtiaga, M. G. Barandika, R. Cortés, S. Martin, L. Lezama, M. I. Arriortua and T. Rojo, *Inorg. Chem.*, 2001, **40**, 4550.
- M.-L. Tong, H. K. Lee, Y.-X. Tong, X.-M. Chen and T. C. W. Mak, *Inorg. Chem.*, 2000, **39**, 4666.
- F. E. Mabbs and D. J. Machin, *Magnetism and Transition Metal Complexes*, Chapman and Hall, London, 1973.
- A. C. T. North, D. C. Phillips and F. S. Mathews, *Acta Crystallogr., Sect. A*, 1968, **24**, 351.
- G. M. Sheldrick, SHELXS-97 Program for X-ray Crystal Structure Solution, University of Göttingen, Germany, 1997.
- G. M. Sheldrick, SHELXL-97 Program for X-ray Crystal Structure Refinement, University of Göttingen, Germany, 1997.
- International Tables for X-ray Crystallography*, Kluwer Academic Publisher, Dordrecht, 1992, vol. C, Tables 4.2.6.8 and 6.1.1.4.
- H. D. Flack, *Acta Crystallogr., Sect. A*, 1983, **39**, 876.
- G. M. Sheldrick, SHELXTL, Version 5, Siemens Industrial Automation Inc., Madison, WI, 1995.
- G. S. Papaefstathiou, A. Escuer, C. P. Raptopoulou, A. Terzis, S. P. Perlepes and R. Vicente, *Eur. J. Inorg. Chem.*, 2001, 1567.
- (a) E. Horn, M. R. Snow and P. C. Zeleny, *Aust. J. Chem.*, 1980, **33**, 1659; (b) S. B. Copp, K. T. Holman, J. O. S. Sangster, S. Subramanian and M. J. Zaworotko, *J. Chem. Soc., Dalton Trans.*, 1995, 2233; (c) M. Herberhold, G. Suss, J. Ellermann and K. Gabelein, *Chem. Ber.*, 1978, **111**, 2931; (d) V. McKee and W. B. Shepard, *J. Chem. Soc., Chem. Commun.*, 1985, 158; (e) L. E. Pence, A. Caneschi and S. J. Lippard, *Inorg. Chem.*, 1996, **35**, 3069.
- (a) F. Schindler, H. Schmidbaur and U. Kruger, *Angew. Chem., Int. Ed. Engl.*, 1965, **4**, 876; (b) H. M. M. Shearer and C. B. Spencer, *Chem. Commun.*, 1966, 194; (c) H. M. M. Shearer and C. B. Spencer, *Acta Crystallogr., Sect. B*, 1980, **36**, 2046; (d) M. M. Olmstead, P. P. Power and S. C. Shoner, *J. Am. Chem. Soc.*, 1991, **113**, 3379; (e) K. Harms, J. Merle, C. Maichle-Mossmer, W. Massa and M. Krieger, *Inorg. Chem.*, 1998, **37**, 1099; (f) S. Lulinski, I. Madura, J. Serwatowski and J. Zachara, *Inorg. Chem.*, 1999, **38**, 4937.
- W. L. Gladfelter, M. W. Lynch, W. P. Schaefer, D. N. Hendrickson and H. B. Gray, *Inorg. Chem.*, 1981, **20**, 2390; M. Schröder, A. J. Blake and A. J. Atkins, *J. Chem. Soc., Chem. Commun.*, 1993, 1662; J. M. Clemente-Juan, B. Chansou, B. Donnadieu and J.-P. Tuchagues, *Inorg. Chem.*, 2000, **39**, 5515.
- A. Escuer, M. Font-Bardia, S. B. Kumer, X. Solans and R. Vicente, *Polyhedron*, 1999, **18**, 909; M. S. E. Fallah, E. Rentschler, A. Caneschi and D. Gatteschi, *Inorg. Chim. Acta*, 1996, **247**, 231.
- K. Y. Ho, W. Y. Yu, K. K. Cheung and C. M. Che, *Chem. Commun.*, 1998, 2101; K. Y. Ho, W. Y. Yu, K. K. Cheung and C. M. Che, *J. Chem. Soc., Dalton Trans.*, 1999, 1581.
- W. Yang, H. Schmidler, Q. Wu, Y.-S. Zhang and S. Wang, *Inorg. Chem.*, 2000, **39**, 2397.
- G. A. Morris, H. Zhou, C. L. Stern and S. T. Nguyen, *Inorg. Chem.*, 2001, **40**, 3222.
- C.-M. Che, C.-W. Wan, K.-Y. Ho and Z.-Y. Zhou, *New J. Chem.*, 2001, **25**, 63; N. W. Alcock, P. R. Barker, J. M. Haider, M. J. Hannon, C. L. Painting, Z. Pikramenou, E. A. Plummer, K. Rissanen and P. Saarenketo, *J. Chem. Soc., Dalton Trans.*, 2000, 1447.